NEOPLASIA
www.neoplasia.com

Volume 11 Number 12 December 2009 pp. 1285–1291 1285

Peptides Derived from Type IV Collagen, CXC Chemokines, and Thrombospondin-1 Domain-Containing Proteins Inhibit Neovascularization and Suppress Tumor Growth in MDA-MB-231 Breast Cancer Xenografts[1,2]

Jacob E. Koskimaki*, Emmanouil D. Karagiannis*, Elena V. Rosca*, Farhad Vesuna†, Paul T. Winnard Jr.†, Venu Raman†, Zaver M. Bhujwalla† and Aleksander S. Popel*

*Department of Biomedical Engineering, School of Medicine, Johns Hopkins University, Baltimore, MD 21205, USA; †Department of Radiology, School of Medicine, Johns Hopkins University, Baltimore, MD 21205, USA

Abstract

Angiogenesis or neovascularization, the process of new blood vessel formation from preexisting microvasculature, involves interactions among several cell types including parenchymal, endothelial cells, and immune cells. The formation of new vessels is tightly regulated by a balance between endogenous proangiogenic and antiangiogenic factors to maintain homeostasis in tissue; tumor progression and metastasis in breast cancer have been shown to be angiogenesis-dependent. We previously introduced a systematic methodology to identify putative endogenous antiangiogenic peptides and validated these predictions *in vitro* in human umbilical vein endothelial cell proliferation and migration assays. These peptides are derived from several protein families including type IV collagen, CXC chemokines, and thrombospondin-1 domain-containing proteins. On the basis of the results from the *in vitro* screening, we have evaluated the ability of one peptide selected from each family named pentastatin-1, chemokinostatin-1, and properdistatin, respectively, to suppress angiogenesis in an MDA-MB-231 human breast cancer orthotopic xenograft model in severe combined immunodeficient mice. Peptides were administered intraperitoneally once per day. We have demonstrated significant suppression of tumor growth *in vivo* and subsequent reductions in microvascular density, indicating the potential of these peptides as therapeutic agents for breast cancer.

Neoplasia (2009) 11, 1285–1291

Introduction

The area of tumor angiogenesis gained attention owing to the pioneering work of Judah Folkman [1], who discovered that neovascular formation was necessary for tumor growth and development. Without a stable blood supply, the tumor would be dependent on oxygen diffusion and be unable to grow past a critical volume or metastasize. The process of neovascular formation involves interactions among several types of cells including endothelial cells, pericytes, vascular smooth muscle cells, parenchymal cells, as well as cell–extracellular matrix interactions. Many growth factors are involved including vascular endothelial growth factor (VEGF), fibroblast growth factor, platelet-derived growth factor, and angiopoietins [2,3].

Abbreviations: HUVECs, human umbilical vein endothelial cells; SCID, severe combined immunodeficient; TSP-1, thrombospondin-1; VEGF, vascular endothelial growth factor

Address all correspondence to: Aleksander S. Popel, Department of Biomedical Engineering, School of Medicine, Johns Hopkins University, 611 Traylor Bldg, 720 Rutland Ave, Baltimore, MD 21205. E-mail: apopel@jhu.edu

[1]The study was supported in part by National Institutes of Health grants R01 CA138264 and R21 CA131931. J.K. was funded through the National Science Foundation Integrative Graduate Education and Research Training Program at Johns Hopkins University, Physical & Biomolecular Foundations for Designing Nanoprobes for Biology, grant no. 0549350.

[2]This article refers to supplementary materials, which are designated by Figures W1 and W2 and are available online at www.neoplasia.com.

Received 14 April 2009; Revised 18 August 2009; Accepted 20 August 2009

 1522-8002/09/$25.00
DOI 10.1593/neo.09620

In normal vascular homeostasis, blood vessels are maintained through a balance of proangiogenic or antiangiogenic factors, whereas pathologies dependent on neovascular development can occur through a resulting imbalance. The progression of solid tumors occurs when a tumor acquires its own blood supply by upregulating proangiogenic factors [4] and is associated with an increase in vascular density [5].

Breast cancer is the most commonly diagnosed female malignancy in the United States, proving fatal to nearly 40,000 people in 2007 with 184,000 additional diagnosed cases [6]. Angiogenesis has been shown to play a key role in breast cancer development, invasion, and metastasis [7–12]. Clinical evidence of angiogenesis in breast cancer is abundant. Intratumoral microvascular density is elevated [5,13], and VEGF expression is increased [13–15] in patients with breast cancer. These factors correlate with a shorter relapse-free and overall survival [16]. Anti-VEGF therapies have shown promise in clinical trials [10] and an anti-VEGF antibody bevacizumab (Roche/Genentech) has been approved by the Food and Drug Administration for breast cancer in 2008 in combination with chemotherapy. Other agents, for example, targeting VEGF receptors, are also in clinical trials [17]. Yet, despite the promise of anti-VEGF therapeutics, it has been suggested that targeting the principal angiogenic factor VEGF alone may never suffice to eradicate malignant tumors, and alternative options should be developed to complement the current VEGF-based therapies with strategies that target other angiogenic factors [2]. It has also been proposed that antiangiogenic therapies may function to stabilize the structurally and functionally abnormal vasculature of the tumor (vascular normalization), resulting in the more effective delivery of chemotherapeutic agents [18].

During the last two decades, a number of endogenous angiogenesis inhibitors have been identified [19–23]. Many of these endogenous inhibitors contain cryptic sites or active sites that are normally hidden from the environment within the protein structure. Once released through proteolytic processing of the proteins, these fragments can act as modulators of neovascular formation. A collection of proteins that constitutes the angiogenesis-inhibiting endogenous regulatory elements exists, balancing the angiogenic switch by counteracting the effects of the various growth factors stimulating angiogenesis [20].

Recently, we have developed a bioinformatics-based approach to identify more than 100 novel putative endogenous antiangiogenic peptides [24]. The peptides are derived from several protein families with localized antiangiogenic properties including type IV collagen, CXC chemokines, and thrombospondin-1 (TSP-1) domain-containing proteins [25–27]. The activity of these peptides and validity of the approach were experimentally verified in several *in vitro* angiogenesis assays, including the migration and proliferation of human umbilical vein endothelial cells (HUVECs). This article describes the application of three selected peptides – one from each family – to an *in vivo* MDA-MB-231 breast cancer orthotopic xenograft model, which resulted in tumor suppression and decreases in microvascular density.

Materials and Methods

In Vitro *Cell Viability Assay Using Human MDA-MB-231 Breast Cancer Cells and Mouse 3T3 Fibroblasts with Application of Peptides Pentastatin-1, Chemokinostatin-1, and Properdistatin*

Cell culture. *In vitro* proliferation assays were completed with each peptide on MDA-MB-231 breast cancer and mouse 3T3 fibroblast cell lines. The MDA-MB-231 cells were acquired from a single donor (ATCC, Manassas, VA). The cells were propagated in RPMI-1640 medium (Cambrex, Walkersville, MD) with 10% FBS and antibiotics (penicillin/streptomycin) under standard conditions of 37°C and 5% CO_2. 3T3 mouse fibroblast cells were acquired from ATCC and grown under standard conditions in Dulbecco's modified Eagle medium (ATCC) with 10% FBS.

Peptide synthesis and handling. The following peptides were synthesized using a solid-phase synthesis technique by a commercial provider (Abgent, San Diego, CA): Pentastatin-1 derived from the α_5 fibril of type IV collagen (both human and mouse sequence: LRRFSTMPFMFCNINNVCNF), chemokinostatin-1 derived from CXCL1 (human sequence used *in vitro* on MDA-MB-231 cells, NGRKACLNPASPIVKKIIEKMLNS; mouse sequence used *in vitro* on 3T3 cells and *in vivo*, NGREACLDPEAPMVQKIVQKMLKG), and properdistatin derived from protein properdin (human sequence, GPWEPCSVTCSKGTRTRRR; mouse sequence, GPWGPCSVTCSKGTQIRQR). Table 1 summarizes the peptide sequences and their proteins of origin. The peptides were stored at temperatures of –80°C. HPLC and mass spectrometry analysis of each peptide were provided by the manufacturer to demonstrate greater than 95% purity. The hydrophobic peptide, pentastatin-1, was solubilized using 10% dimethyl sulfoxide (DMSO) without any demonstrated effect on cell viability. Chemokinostatin-1 and properdistatin were solubilized in PBS before use.

In vitro *cell viability assay.* The antitumor effects of the peptides on the MDA-MB-231 cell line were measured using the colorimetric cell proliferation reagent WST-1 (Roche, Indianapolis, IN). Approximately 2×10^3 cells were seeded per well in a 96-well microplate and were exposed for 3 days to several different peptide concentrations of 1, 10, 20, 30, 40, 50, 80, and 100 μg/ml. Cells were tested in quadruplicate for each concentration. As an experimental control, equivalent to normal cell viability, the cells were cultured without any agent in complete medium containing growth factors and serum without any exposure to peptide. Effects on the viability of 3T3 fibroblasts were conducted in a similar fashion with peptides applied at the same concentrations.

Table 1. Amino Acid Sequences of the Tested Peptides.

Peptide Name	Peptide Origin	Accession No.	Peptide Sequence (Human/Mouse)
Pentastatin-1	α_5 fibril of collagen IV	AAF66217 (1516-1535)	LRRFSTMPFMFCNINNVCNF LRRFSTMPFMFCNINNVCNF
Chemokinostatin-1	CXCL1/Gro-α	P00341 (80-103)	NGRKACLNPASPIVKKIIEKMLNS NGREACLDPEAPMVQKIVQKMLKG
Properdistatin	Properdin	AAB63280.1 (143-161)	GPWEPCSVTCSKGTRTRRR GPWGPCSVTCSKGTQIRQR

Statistical analysis. Statistical significance for *in vitro* results was assessed using the Student's *t*-test, with $P < .01$ defined as significant. *In vivo* results were tested using both the Student's *t*-test at $P < .05$ and the nonparametric Wilcoxon rank sum test. Peptides were compared with the experimental control and scrambled peptide equivalent. Tumor volumes were measured on days 1, 4, 7, 10, and 13, and the average tumor size per condition was reported over time. The SEM is reported.

Translation from in vitro *to selected* in vivo *peptides.* On the basis of our previous *in vitro* results [25–27], we selected one peptide with both significant antiproliferative and antimigratory activity from three dominant peptide families: type IV collagen, CXC chemokines, and TSP-1 domain-containing peptides to test *in vivo* in breast xenografts.

In vivo *tumor xenograft models.* Animal protocols were approved by the Institutional Care and Use Committee at the Johns Hopkins Medical Institutions (JHMI). A population of MDA-MB-231 breast cells were washed twice in PBS and gently resuspended in RPMI medium to generate a single cell suspension. Subsequently, the cells were injected into the mammary fat pad of severe combined immunodeficient (SCID) mice at a concentration of 2 million cells/100-μl solution. After growth incubation of 14 to 21 days, tumor volumes were calculated from measurements of tumor dimensions with calipers. Tumor growth was monitored to an initial average size of 75 to 100 mm^3, which usually developed within 21 days after inoculation. Peptides were administered once per day, intraperitoneally, in doses of 10 mg/kg for pentastatin-1, and 20 mg/kg for chemokinostatin-1 and properdistatin. The more hydrophobic peptide, pentastatin-1, was dissolved in 10% DMSO and 90% H_2O to ensure solubility before administration. Equivalent volumes of PBS solution were injected as an experimental control. Separate controls of scrambled peptide sequences were also made for each peptide tested to provide proof that the antiangiogenic efficacy of the novel peptides was sequence-dependent. The injections were continued for 13 days with a total of eight animals per group used for each condition.

Immunohistochemistry. Immediately after the sacrifice of mice, tumors were excised and stored in a zinc-based fixative (BD Biosciences, San Jose, CA) for 10 to 14 days and processed by the JHMI Immunohistochemistry Core Facility. Paraffin sections of 5 μm were obtained from the central cross-sectional volume of each tumor. After deparaffinization and rehydration, the sections were treated overnight with a monoclonal rat antimouse CD31 platelet endothelial cell adhesion molecule immunoglobulin G antibody (BD PharMingen, San Jose, CA), which specifically recognizes an epitope on the surface of endothelial cells. Each tumor section was also subsequently processed and stained using hematoxylin-eosin (H&E) stain to visualize tissue structure and core necrotic regions in the tumor. Histologic samples were processed using Aperio Image Scope Software (Aperio Technologies, Inc, Vista, CA), quantified using FRiDA software (Johns Hopkins University, Baltimore, MD), and scaled as a percentage of the experimental control. Each peptide was compared with the experimental control and scrambled peptide equivalent using the Student's *t*-test at $P < .05$.

Additional staining was made to assess the origin and proliferation status of single cells within the tumor microenvironment using fluorescence costaining for telomeric DNA to differentiate human from murine cells and the proliferative marker Ki67 (Figure 5) by the JHMI Immunohistochemistry Core Facility as previously described [28]. Briefly, deparaffinized slides were processed with citrate buffer (Vector Laboratories, Burlingame, CA), placed in PBS with Tween (Sigma, St Louis, MO), followed by ethanol, and then air-dried. Slides were then treated with 25 μl of a Cy3-labeled telomere-specific peptide nucleic acid (PNA) at 0.3 μg/ml PNA in 70% formamide, 10 mM Tris, pH 7.5, 0.5% B/M blocking reagent (catalog no. 1814-320; Boehringer-Mannheim, Indianapolis, IN). Slides were then further processed for indirect immunofluorescence by application of primary antibody (anti-Ki67, catalog no. NCL-Ki67p, diluted 1:1200; Novocastra Laboratories, Newcastle upon Tyne, UK) followed by application of the goat antirabbit IgG fraction Alexa Fluor 488 fluorescent secondary antibody (catalog no. A-11001, diluted 1:100; Molecular Probes, Invitrogen, Carlsbad, CA). Next, nuclei were counterstained with 4′-6-diamidino-2-phenylindole (DAPI) at 500 ng/ml in deionized water (catalog no. D-8417; Sigma Chemical Co). The PNA probe complementary to the mammalian telomere repeat sequence was obtained from Applied Biosystems (Framingham, MA) and has the sequence (N-terminus to C-terminus) CCCTAACCCTAACCCTAA with an N-terminal covalently linked Cy3 fluorescent dye.

Slides were imaged with a Nikon 50i epifluorescence microscope equipped with X-cite series 120 illuminator (EXFO Photonics Solutions, Inc, Ontario, Canada) and a 100×/1.4 NA oil immersion Neofluar lens. Fluorescence excitation/emission filters were as follows: Cy3 excitation, 546 nm/10 nm BP; emission, 578 nm LP (Carl Zeiss Inc, Germany); DAPI excitation, 330 nm; emission, 400 nm through an XF02 fluorescence set (Omega Optical, Brattleboro, VT); Alexa Fluor 488 excitation, 475 nm; emission, 535 nm through a combination of 475RDF40 and 535RDF45 filters (Omega Optical). Signal capture ranged from 16 milliseconds for the DAPI counterstain, 510 milliseconds for fluorescein isothiocyanate (centromere), and 200 milliseconds for Cy3 (telomere) with six images taken per condition. Images were then processed using Image J software (US National Institutes of Health, Bethesda, MD) to preserve fluorescence intensity. Images were then overlain and compiled using Adobe Photoshop CS3 Software (Adobe Systems, Inc, San Jose, CA). Pixel intensity and cell counts were also approximated using Adobe Photoshop.

Results

Endothelial cells, tumor cells, and surrounding fibroblasts can all be sensitive to peptide inhibitors. *In vitro* viability experiments were conducted on two different cell lines, MDA-MB-231 breast tumor cells and mouse 3T3 fibroblasts, after 3 days of incubation with peptide. Figure 1 shows the dose-response of pentastatin-1 applied to MDA-MB-231 tumor cells, showing maximal activity at concentrations greater than 50 μg/ml, and 3T3 fibroblasts, showing maximal activity at concentrations greater than 40 μg/ml. There were no significant differences between peptide-treated wells and the experimental control shown in both cell lines for chemokinostatin-1 and properdistatin (data not shown), although they have been previously shown to inhibit the migration and proliferation of HUVECs [24,26,27].

Once *in vitro* studies were completed, each peptide was administered intraperitoneally to MDA-MB-231 xenograft-bearing mice. Mice were inoculated with 2×10^6 cells/100 μl, and tumors were allowed to grow for 14 to 21 days until reaching an average volume of 75 to 100 mm^3. Each condition contained $n = 8$ animals and was compared with an experimental PBS-treated control, shown in Figure 2. In a separate experiment, 10% DMSO and PBS-treated controls were tested to show if there was no significant difference due to DMSO (data not shown). Scrambled peptide controls were also tested and showed no significant difference from the PBS- or DMSO-treated controls at any day (data not shown). Pentastatin-1 treatment resulted in a significant tumor

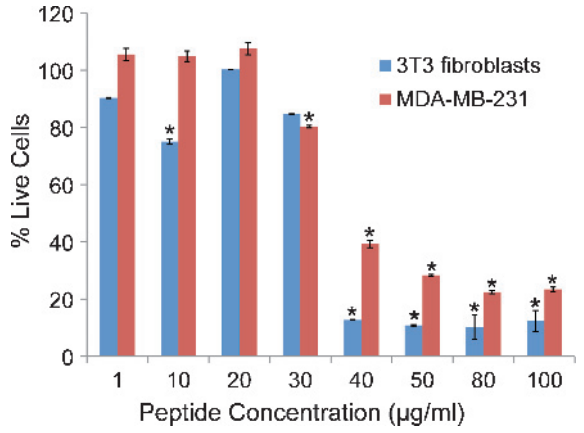

Figure 1. *In vitro* proliferation results for pentastatin-1 on MDA-MB-231 breast tumor cells and 3T3 fibroblasts. Cell viability was determined using a WST-1 colorimetric assay at the end of a 72-hour exposure to peptide. Data are scaled so that 100% represents the signal from the experimental control and thus maximum viability. Cells were treated at concentrations of 1, 10, 20, 30, 40, 50, 80, and 100 μg/ml of peptide. Pentastatin-1, at high concentrations, decreased viability of 3T3 fibroblasts and MDA-MB-231 breast cancer cell lines *in vitro* in this assay. Statistical significance is determined at $P < .01$, and the vertical error bars represent the SEM.

growth suppression throughout the duration of the experiment as determined by the Student's *t*-test and the Wilcoxon statistical analysis except for day 7 when only the Student's *t*-test showed significance. Nonetheless, differences in tumor growth were significant for the remainder of the experiment compared with the experimental control. Chemokinostatin-1 treatment also resulted in a significant suppression of tumor growth compared with the experimental control, with the exception of day 13 for which the Wilcoxon statistical analysis and the Student's *t*-test both showed a nonsignificant result. In this case, tumor volumes at days 10 and 13 were also not significantly different compared with the scrambled peptide equivalent. Properdistatin-treated tumors showed a significant volume change from the PBS controls and scrambled peptide treated throughout the duration of the experiment by both the Student's *t*-test and the Wilcoxon test. As shown in Figure 2*B*, by day 13, tumors in the experimental control group had grown by an average of 275% from starting values at the onset of injections, whereas pentastatin-1–treated tumors increased by 150%, chemokinostatin-1–treated tumors increased by 170%, and properdistatin-treated tumors increased by 153%. Throughout the duration of the experiment, toxicity was monitored by weight changes in the mice, and peptide-treated groups were shown to have no statistically significant change from the control. Additional H&E staining of vital organ sections including lung, liver, and kidney showed no abnormal pathologies in any condition, summarized in Figure W1.

Figure 3 shows H&E staining from the experimental control and peptide-treated tumors at 1× and 2× magnifications. It can be seen that the pentastatin-1– and properdistatin-treated tumors have increased central necrosis in the tumor microenvironment as indicated by arrows on the photomicrographs. Chemokinostatin-1–treated tumors appeared to be similar to the control group with less necrotic areas. Immunohistochemistry was also performed on tumor xenografts postmortem after tumors had been fixed in zinc-containing solution and stained with a CD31 antibody, a common marker for vessels and endothelial cells. Figure 4*A* shows decreases in vascularization in pentastatin-1–, chemokinostatin-1–, and properdistatin-treated tumors at 20× magnification as indicated by the lower amount of CD31 staining. Figure 4*B* shows microvascular density quantification for each peptide based on endothelial cell staining by CD31. Results for scrambled peptide equivalents were not significantly different from the respective experimental controls. Pentastatin-1 had a significant decrease in vessel density in comparison to the experimental control, whereas chemokinostatin-1 showed a decrease in microvascular density in comparison to both the experimental control and its scrambled peptide equivalent. Properdistatin also showed some reduction in vascular density from its scrambled peptide equivalent and experimental control, although the results were not statistically significant.

Figure 5*A* shows the results of fluorescence costaining for Ki67 proliferating cells (*green*) and mouse cells (*red*). DAPI (*blue*), which specifically stains cell nuclei, was used for estimating cell numbers as shown in the composite images (*left panel*). Qualitatively, the peptide-treated tumors show a reduction in proliferating cells for pentastatin-1, chemokinostatin-1, and properdistatin at the time of termination and fixation. Figure 5*B* shows the quantification of the fluorescence in the photomicrographs of Figure 5*A* as an estimate of the number of proliferating cells and mouse stromal cell composition in the tumors. The controls show on average 38% proliferating cells in the tumor and 21% mouse stromal cells. Pentastatin-1 and chemokinostatin-1 show 16% and 26% proliferating cells, respectively, whereas properdistatin shows a statistically lower percentage at 14%. The percentages of mouse stromal cells in pentastatin-1 and properdistatin are not statistically different from

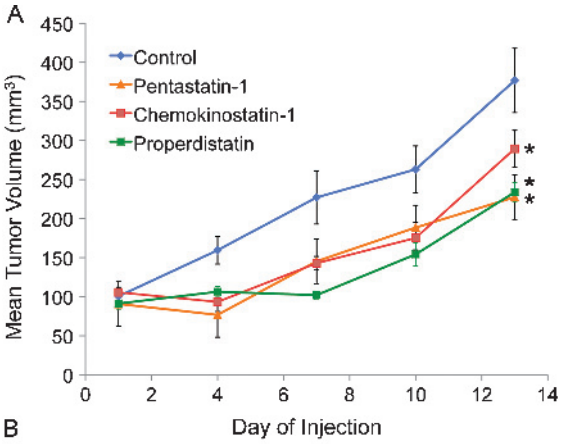

Condition	Day 4	Day 7	Day 10	Day 13
Control	59	126	162	275
Pentastatin-1	-16	60	108	151
Chemokinostatin-1	-12	35	66	174
Properdistatin	15	11	67	153

Figure 2. (A) MDA-MB-231 breast xenograft growth in SCID mice with application of three peptides derived from three protein families. Cells were inoculated orthotopically into the mammary fat pad with 2×10^6 cells/mouse, and tumors were allowed to grow for 14 to 21 days to an average of 75 to 100 mm^3 on peptide administration. The average tumor volume ($n = 8$) is plotted every fourth day after treatment. Tumor volumes are statistically different from the control at $P < .05$ by Student's *t*-test for all days except chemokinostatin-1 on day 13. Scrambled peptide equivalents were also tested *in vivo* and were not statistically different from the experimental control. (B) Tumor percent change is also shown from the starting tumor values on peptide administration.

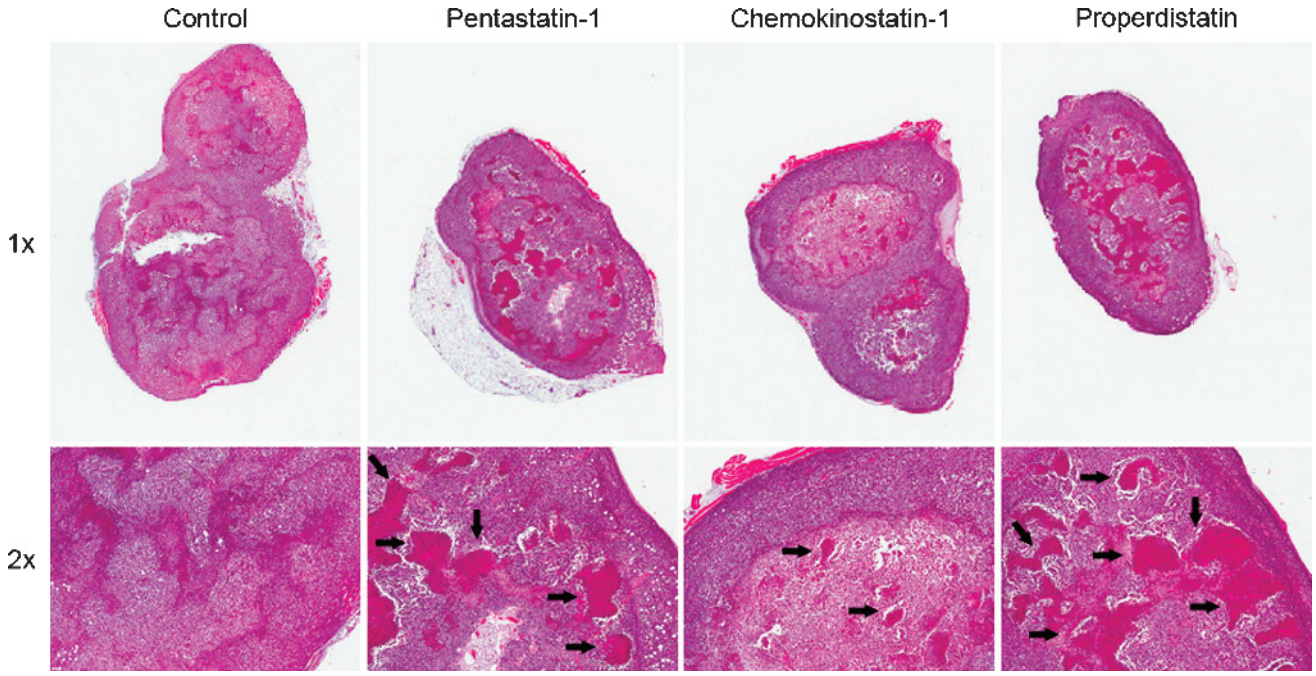

Figure 3. H&E staining of tumor cross sections at 1× and 2× for the experimental control, pentastatin-1, chemokinostatin-1, and properdistatin. Pentastatin-1– and properdistatin-treated tumors show increased necrotic regions (arrows), whereas chemokinostatin-1 is most similar to the control.

the control, whereas the chemokinostatin-1–treated tumors show a marked 67% stromal cell fraction in the tumor microenvironment.

Discussion

Endogenous peptides with antiangiogenic activity have emerged as one of the leading tools to treat cancer in addition to polypeptides, small molecules, and antibodies [29]. We have previously introduced a systematic methodology for the identification of antiangiogenic peptide sequences and demonstrated that a high percentage of the predicted peptides indeed inhibit the proliferation and migration of HUVECs *in vitro*. On the basis of this *in vitro* screening, we selected one molecule from three protein classes—pentastatin-1, a collagen IV–derived peptide; chemokinostatin-1, a CXC chemokine–derived peptide; and properdistatin, a TSP-1 domain-containing peptide—and tested them *in vitro* on additional cell lines and *in vivo* in an orthotopic MDA-MB-231 breast xenograft model.

We demonstrated *in vitro* that pentastatin-1 has anticellular effects on MDA-MB-231 cells and decreases 3T3 fibroblast viability; however, chemokinostatin-1 and properdistatin do not exhibit these effects. The latter peptides have been previously shown to exhibit antiproliferative and antimigratory properties on HUVECs [26,27]. Pentastatin-1 has also been previously shown to inhibit proliferation and migration of endothelial cells *in vitro* [25], and we demonstrated inhibition of tumor growth *in vivo*. Supplementary flow cytometry data in Figure W2 show receptor identification of β_1-integrins for MDA-MB-231 cells. Pentastatin-1 has been previously shown to bind to β_1-integrins [24], which we show are present in high percentages for both HUVECs at 85% of cells and MDA-MB-231 at 79% of cells, indicating that the peptide is capable of directly inhibiting tumor cell proliferation in addition to being antiangiogenic. Chemokinostatin-1 was similarly shown to bind to CXCR3 through antibody neutralization experiments, and properdistatin was shown to bind to the CD36 receptor [24]. Both of these peptides inhibit the proliferation of HUVECs; however, they did not inhibit tumor cell proliferation or proliferation of 3T3 fibroblasts. Flow cytometry data indicate a low percentage of these receptors in MDA-MB-231 cells, suggesting that the activity of these peptides is likely monomodal and localized only to proliferating endothelial cells.

The three endogenous peptides show significant tumor suppression at the concentrations of 10 mg/kg for pentastatin-1 and 20 mg/kg for both chemokinostatin-1 and properdistatin. The scrambled peptide controls strongly suggest the efficacy of the peptides is sequence-dependent. Although randomly mutating peptide amino acid sequences does not guarantee the resulting sequence will not retain some binding interactions among receptor families, in this case the scrambled sequences only retain nominal activity, which was not statistically significant from the experimental controls.

Immunohistochemistry was performed using the CD31 antibody, which is specific for endothelial cells. In pentastatin-1– and chemokinostatin-1–treated tumors, there is a statistically significant inhibition of endothelial cells and a reduction in microvessel volume, indicating that the peptides are antiangiogenic. Chemokinostatin-1–treated tumors grew more rapidly toward the end of the experiment, indicating possible endothelial cell resistance to the peptide. In our H&E staining of tumor cross sections on day 13, we found that chemokinostatin-1 is most similar to the experimental control, containing minimal core necrotic regions, suggesting the peptide's less deleterious effect on the tumor microenvironment. We also show that in chemokinostatin-1–treated mice, their tumors have a higher percentage of proliferating cells than the pentastatin-1– or properdistatin-treated tumors. The significant quantity of mouse stromal cells suggests a high infiltration of these cells into the tumor microenvironment owing to the presence of the chemokine-derived peptide. Chemokinostatin-1 is notably derived from the proangiogenic ELR-positive CXC chemokines. The cancer biology of CXC chemokines is complex because these

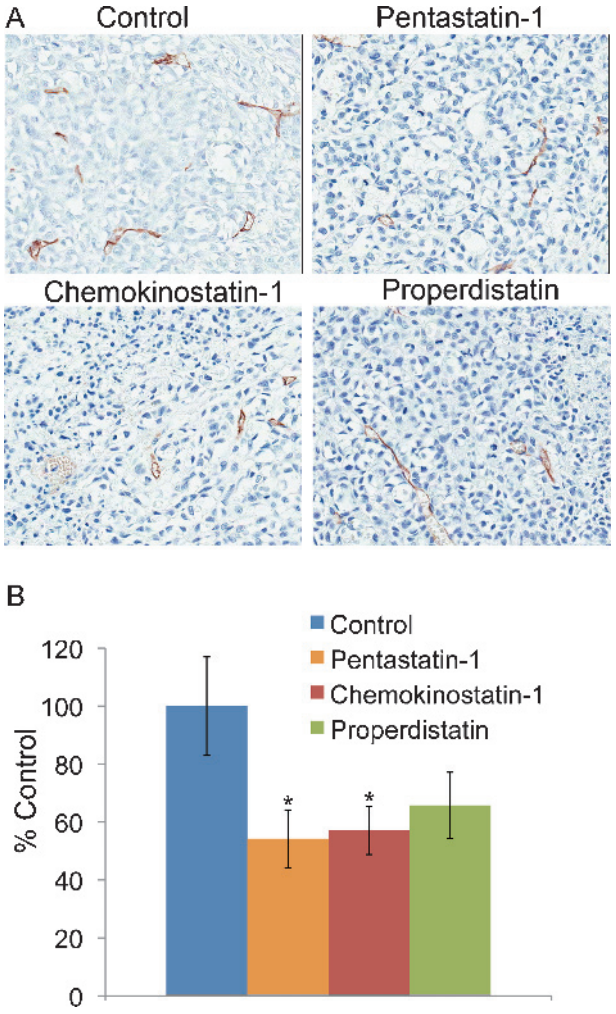

Figure 4. (A) Immunohistochemistry showing CD31 antibody staining in several conditions as a marker for endothelial cells and vessel density. Images were taken at 20× magnification for the experimental control, pentastatin-1–, chemokinostatin-1–, and properdistatin-treated tumors. (B) Quantification of endothelial cells and vessel density for resulting cross sections scaled to the experimental control. Each condition was quantified by pixel intensity representing the quantity of endothelial cells. The type IV collagen–derived peptide, pentastatin-1, and CXC chemokine–derived peptide, chemokinostatin-1, were statistically different from the control at $P < .05$. Chemokinostatin-1 was also statistically significant from its scrambled peptide control, showing a reduction in endothelial cells and vasculature.

peptides may stimulate the infiltration of various stromal cells into the tumor microenvironment [30]. Although the SCID mice used in this experiment lack T and B lymphocytes, there may be an influx of other mouse stromal cells into the tumor owing to the presence of the chemokine-derived peptide.

The experiments were terminated after day 13 of treatment because some peptide-treated tumors had begun to escape and grew as rapidly as the controls, indicating tumor resistance to the applied peptides. Recently, it has been proposed that there can be at least two underlying mechanisms for resistance to antiangiogenic therapies: adaptive or evasive resistance and intrinsic nonresponsiveness [31]. On the basis of the initial response phase of peptide treatment we observed in the case of each peptide, we hypothesize a form of adaptive resistance developed within the tumor microenvironment in response to the peptide treatment. Recent systematic investigation of resistance to endogenous antiangiogenic agents (TSP-1, endostatin, and tumstatin) demonstrates that tumors escape the treatments after several days, and a number of proangiogenic factors (e.g., VEGF, FGF-2, transforming growth factor-β) are upregulated [4]. Other general mechanisms of resistance include the recruitment of bone marrow–derived proangiogenic cells, increased pericyte coverage in the tumor vasculature, and increased activation of invasion and metastasis for access to normal tissue vasculature [31]. Future studies should be performed to determine the modes of

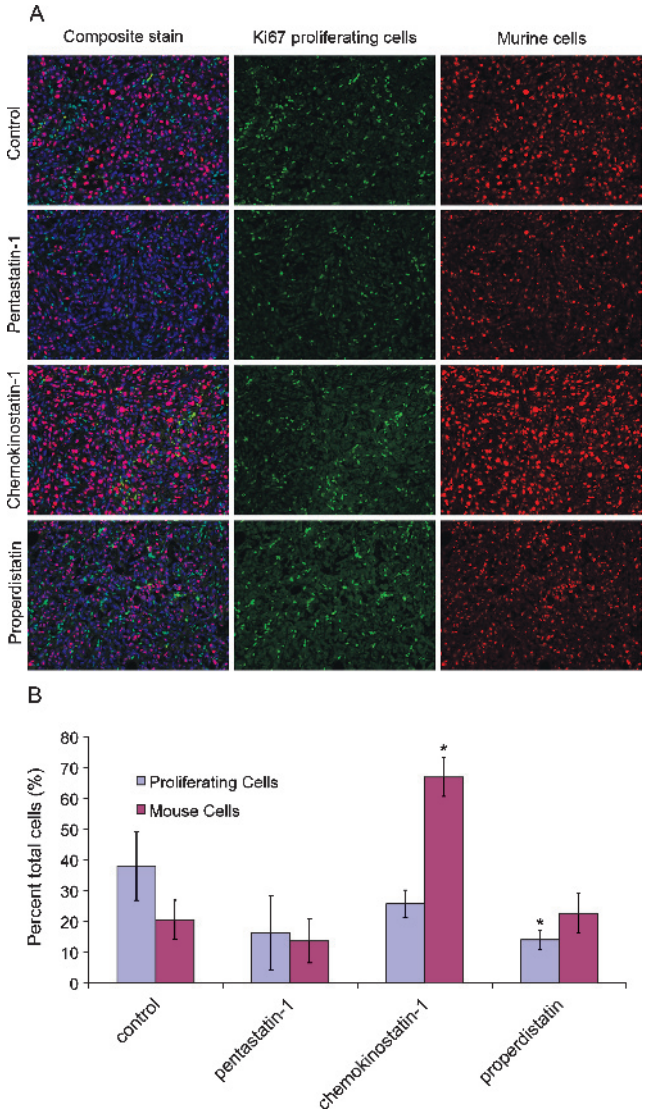

Figure 5. (A) Fluorescence costain for Ki67 proliferating cells (green) and murine cells by telomeric DNA (red). Composite images are made with DAPI (blue) as a stain for cell nuclei (left panel). Cell counts are approximated using pixel intensity with Image J and Adobe Photoshop CS3 software. Qualitatively, the pentastatin-1–, chemokinostatin-1–, and properdistatin-treated tumors contain fewer proliferating cells than the control. (B) Quantification of proliferating cells and mouse stromal cells. Controls contained an average of 38% proliferating cells and 21% mouse stromal cells. Properdistatin contained a statistically significant reduction in proliferating cells with 14% proliferating. Chemokinostatin-1 contained a statistically significant increase in mouse stromal cells from the controls, with 67% of the tumor microenvironment of this type, suggesting an infiltration of murine-derived cells into the tumor microenvironment.

resistance for each peptide and whether treatment efficacy can be further sustained. Despite these initial limitations, the peptides have a potential to regulate and suppress vessel growth *in vivo* and in translational studies possibly when combined with cytotoxic agents or in combinations with other antiangiogenic agents.

Breast cancer has been shown to be angiogenesis-dependent; thus, advances in the development of antiangiogenic agents should contribute to the arsenal of therapeutic tools available for treatment of the disease. The presented results indicate the selected peptides may have the potential for translational clinical therapeutics in breast cancer. In summary, we have demonstrated that systematically identified peptides derived from type IV collagen, CXC chemokines, and TSP-1 inhibit neovascularization in MDA-MB-231 breast xenografts and are candidates for translational therapeutics in breast cancer.

Acknowledgments

The authors thank Amina A. Qutub for her advice and experimental assistance and Antonio C. Wolff and Rezina Siddique for useful discussion.

References

[1] Folkman J (1971). Tumor angiogenesis: therapeutic implications. *N Engl J Med* **285**, 1182–1186.

[2] Carmeliet P (2005). Angiogenesis in life, disease and medicine. *Nature* **438**, 932–936.

[3] Carmeliet P and Jain RK (2000). Angiogenesis in cancer and other diseases. *Nature* **407**, 249–257.

[4] Fernando NT, Koch M, Rothrock C, Gollogly LK, D'Amore PA, Ryeom S, and Yoon SS (2008). Tumor escape from endogenous, extracellular matrix–associated angiogenesis inhibitors by up-regulation of multiple proangiogenic factors. *Clin Cancer Res* **14**, 1529–1539.

[5] Uzzan B, Nicolas P, Cucherat M, and Perret GY (2004). Microvessel density as a prognostic factor in women with breast cancer: a systematic review of the literature and meta-analysis. *Cancer Res* **64**, 2941–2955.

[6] Jemal A, Siegel R, Ward E, Hao Y, Xu J, Murray T, and Thun MJ (2008). Cancer statistics, 2008. *CA Cancer J Clin* **58**, 71–96.

[7] Banerjee S, Dowsett M, Ashworth A, and Martin LA (2007). Mechanisms of disease: angiogenesis and the management of breast cancer. *Nat Clin Pract Oncol* **4**, 536–550.

[8] Doyle DM and Miller KD (2008). Development of new targeted therapies for breast cancer. *Breast Cancer* **15**, 49–56.

[9] Hayes DF, Miller K, and Sledge G (2007). Angiogenesis as targeted breast cancer therapy. *Breast* **16** (Suppl 2), S17–S19.

[10] Salter JT and Miller KD (2007). Antiangiogenic agents in breast cancer. *Cancer Invest* **25**, 518–526.

[11] Schneider BP and Miller KD (2005). Angiogenesis of breast cancer. *J Clin Oncol* **23**, 1782–1790.

[12] Schneider BP and Sledge GW Jr (2007). Drug insight: VEGF as a therapeutic target for breast cancer. *Nat Clin Pract Oncol* **4**, 181–189.

[13] Guidi AJ, Schnitt SJ, Fischer L, Tognazzi K, Harris JR, Dvorak HF, and Brown LF (1997). Vascular permeability factor (vascular endothelial growth factor) expression and angiogenesis in patients with ductal carcinoma *in situ* of the breast. *Cancer* **80**, 1945–1953.

[14] Kut C, Mac Gabhann F, and Popel AS (2007). Where is VEGF in the body? A meta-analysis of VEGF distribution in cancer. *Br J Cancer* **97**, 978–985.

[15] Relf M, LeJeune S, Scott PA, Fox S, Smith K, Leek R, Moghaddam A, Whitehouse R, Bicknell R, and Harris AL (1997). Expression of the angiogenic factors vascular endothelial cell growth factor, acidic and basic fibroblast growth factor, tumor growth factor beta-1, platelet-derived endothelial cell growth factor, placenta growth factor, and pleiotrophin in human primary breast cancer and its relation to angiogenesis. *Cancer Res* **57**, 963–969.

[16] Sachdev JC and Jahanzeb M (2008). Evolution of bevacizumab-based therapy in the management of breast cancer. *Clin Breast Cancer* **8**, 402–410.

[17] Choueiri TK (2008). Axitinib, a novel anti-angiogenic drug with promising activity in various solid tumors. *Curr Opin Investig Drugs* **9**, 658–671.

[18] Jain RK (2008). Lessons from multidisciplinary translational trials on anti-angiogenic therapy of cancer. *Nat Rev Cancer* **8**, 309–316.

[19] Clamp AR and Jayson GC (2005). The clinical potential of antiangiogenic fragments of extracellular matrix proteins. *Br J Cancer* **93**, 967–972.

[20] Folkman J (2007). Angiogenesis: an organizing principle for drug discovery? *Nat Rev Drug Discov* **6**, 273–286.

[21] Nakamura T and Matsumoto K (2005). Angiogenesis inhibitors: from laboratory to clinical application. *Biochem Biophys Res Commun* **333**, 289–291.

[22] Nyberg P, Xie L, and Kalluri R (2005). Endogenous inhibitors of angiogenesis. *Cancer Res* **65**, 3967–3979.

[23] Volpert OV (2000). Modulation of endothelial cell survival by an inhibitor of angiogenesis thrombospondin-1: a dynamic balance. *Cancer Metastasis Rev* **19**, 87–92.

[24] Karagiannis ED and Popel AS (2008). A systematic methodology for proteome-wide identification of peptides inhibiting the proliferation and migration of endothelial cells. *Proc Natl Acad Sci USA* **105**, 13775–13780.

[25] Karagiannis ED and Popel AS (2007). Identification of novel short peptides derived from the α_4, α_5, and α_6 fibrils of type IV collagen with anti-angiogenic properties. *Biochem Biophys Res Commun* **354**, 434–439.

[26] Karagiannis ED and Popel AS (2008). Novel anti-angiogenic peptides derived from ELR-containing CXC chemokines. *J Cell Biochem* **104**, 1356–1363.

[27] Karagiannis ED and Popel AS (2007). Anti-angiogenic peptides identified in thrombospondin type I domains. *Biochem Biophys Res Commun* **359**, 63–69.

[28] Meeker AK, Gage WR, Hicks JL, Simon I, Coffman JR, Platz EA, March GE, and De Marzo AM (2002). Telomere length assessment in human archival tissues: combined telomere fluorescence *in situ* hybridization and immunostaining. *Am J Pathol* **160**, 1259–1268.

[29] Ruegg C, Hasmim M, Lejeune FJ, and Alghisi GC (2006). Antiangiogenic peptides and proteins: from experimental tools to clinical drugs. *Biochim Biophys Acta* **1765**, 155–177.

[30] Vandercappellen J, Van Damme J, and Struyf S (2008). The role of CXC chemokines and their receptors in cancer. *Cancer Lett* **267**, 226–244.

[31] Bergers G and Hanahan D (2008). Modes of resistance to anti-angiogenic therapy. *Nat Rev Cancer* **8**, 592–603.

Supporting Information

Supporting Materials and Methods

Fixation of vital organs. Severe combined immunodeficient mice with MDA-MB-231 breast xenografts were humanely killed after 13 days of treatment with peptides or PBS using CO_2. Liver, lungs, and kidneys were excised and stored in zinc-based fixative (BD Biosciences) for 3 weeks, after which samples were placed in paraffin blocks. H&E staining was made to visualize tissue structure for pathology and normal tissue structure in comparison to the experimental control. Histologic samples were processed using Aperio Image Scope Software (Aperio Technologies) and compiled using Adobe Photoshop CS3 Software (Adobe Systems).

Flow cytometry analysis for receptor identification. Flow cytometry analysis was completed for receptor quantification on primary HUVECs and MDA-MB-231 breast cancer cells. HUVECs were acquired from a single donor were purchased from Cambrex. Cells were propagated in endothelial growth medium-2 (Lonza, Basel, Switzerland) using 2% FBS, growth factors (human basic fibroblast growth factor and VEGF), and antibiotics (gentamicin/amphotericin B). All cells used were from passage 3 to passage 6. MDA-MB-231 breast cancer cells were acquired from a single donor (ATCC) as described previously and propagated in RPMI-1640 medium (Cambrex) with 10% FBS and antibiotics (penicillin/streptomycin). Cells were gently dissociated from their flasks using PBS/EDTA (200 mg/ml), counted, and aliquoted at 5×10^5 cells/ml in medium. Heat-aggregated human IgG at 20 μg/ml was used to block nonspecific binding. Medium containing different monoclonal antibody solutions at 20 μl/1 × 10^6 cells were applied for β_1-integrins (FAB17781; R&D Systems, Minneapolis, MN), CXCR3 (FAB1685; R&D Systems), and CD36 (CB38/NL07; BD PharMingen). Cells were then incubated for 60 minutes at 4°C to allow binding of receptors to antibody, pelleted after centrifuging at 1000 RPM for 5 minutes at 4°C, and washed with a 200-μl medium of 1% FBS three times. Three hundred microliters of buffer (PBS, 1% BSA, 0.1% NaN_3; Sigma-Aldrich, Inc) was applied and transferred to FACS tubes. Flow cytometry analysis and protocols were followed using the FACSCalibur (BD Biosciences), and receptors were quantified using FlowJo Flow Cytometry Analysis Software (Tree Star, Inc, Ashland, OR).

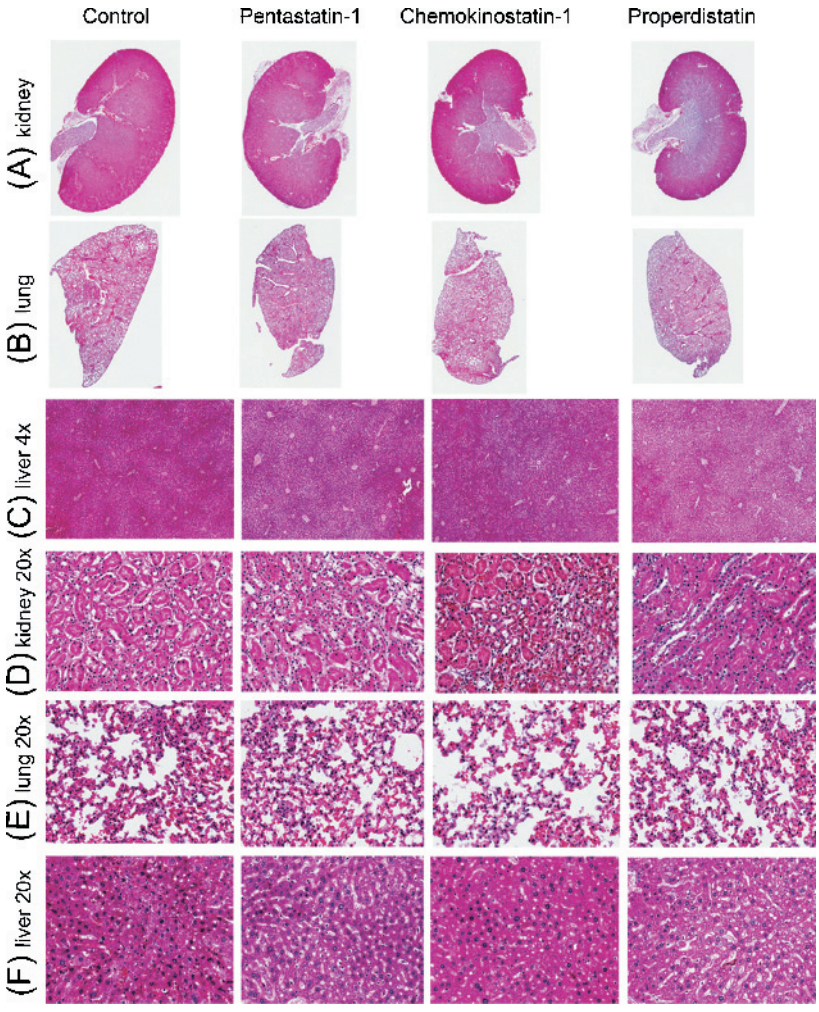

Figure W1. Peptide-treated tumors and their respective vital organs using H&E staining on day 13. Gross tissue morphology is shown in (A) for kidney at 1×, and (B) normal lung structure at 1×. (C) Liver sections were taken and magnified at 4× to show consistent morphology in control and peptide-treated tumors. (D) Kidney, (E) lung, and (F) liver were magnified at 20× to show normal cell structure and the absence of pathologies due to peptide delivery.

A

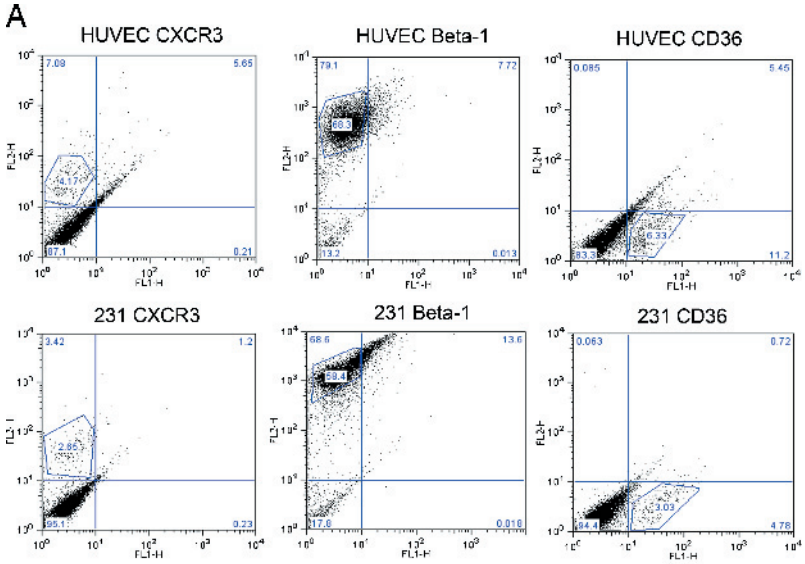

B

Receptor	Cell Type	Quadrant	Event	% Gated	Ratio (HUVEC/231)
Beta-1	HUVEC	UL	4165	84.5	1.1
	231	UL	5052	78.8	
CXCR3	HUVEC	UL	272	5.3	1.9
	231	UL	86	2.7	
CD36	HUVEC	LR	316	4.4	1.5
	231	LR	92	2.9	

Figure W2. Flow cytometry analysis for receptor identification on HUVECs and MDA-MB-231 cells. (A) Phycoerythrin conjugation for CXCR3 identification on HUVECs and MDA-MB-23s, showing 5.3% cells contain the receptor in HUVECs and 2.9% in MDA-MB-23s. Similar analysis shows HUVECs contain the β_1-integrin receptor in 84.5% of cells, and 78.8% of MDA-MB-231 cells. Fluorescein isothiocyanate conjugation for CD36 revealed 4.4% of HUVECs and 2.9% of MDA-MB-231 cells contain the receptor. (B) The corresponding table summarizes the ratios of these receptors in HUVEC/MDA-MB-231 cells as 1.9 for CXCR3, 1.1 for β_1-integrins, and 1.5 for CD36.